Macromolecules

Article

pubs.acs.org/Macromolecules

Synthesis, Light Emission, Explosive Detection, Fluorescent Photopatterning, and Optical Limiting of Disubstituted Polyacetylenes Carrying Tetraphenylethene Luminogens

Carrie Y. K. Chan,[†,‡] Jacky W. Y. Lam,[†,‡] Chunmei Deng,[†,‡] Xiaojun Chen,[‡] Kam Sing Wong,[‡] and Ben Zhong Tang*[,†,‡,§]

[†]HKUST-Shenzhen Research Institute, No. 9 Yuexing 1st RD, South Area, Hi-tech Park, Nanshan, Shenzhen 518057, China

[‡]Department of Physics, Department of Chemistry, Division of Life Science, State Key Laboratory of Molecular Neuroscience, Institute for Advanced Study, Institute of Molecular Functional Materials, Division of Biomedical Engineering, The Hong Kong University of Science and Technology, Clear Water Bay, Kowloon, Hong Kong, China

[§]Guangdong Innovative Research Team, SCUT-HKUST Joint Research Laboratory, State Key Laboratory of Luminescent Materials and Devices, South China University of Technology, Guangzhou 510640, China

Supporting Information

ABSTRACT: Tetraphenylethene-functionalized acetylenes [$(C_6H_5)_2C{=}C(C_6H_5)(C_6H_4C{\equiv}CR)$, R = C_8H_{17} and C_6H_5] were synthesized, and their polymerizations were effected by WCl_6–Ph_4Sn at elevated temperatures in toluene under nitrogen, furnishing polymers **P1** and **P2**. The polymers possessed good solubility and degraded at high temperatures of up to ~400 °C under nitrogen. Both polymers emitted weakly in the solution state. Whereas the emission of **P1** was enhanced when aggregated, that of **P2** was quenched, demonstrating that the light emission of polyacetylenes could be varied readily by changing their molecular structure. The polymers could serve as fluorescent chemosensors for explosive detection with an amplification effect. UV irradiation of their films in air photo-oxidized and bleached the fluorescence of the exposed parts, generating fluorescent photopatterns. The polymers exhibited optical nonlinearity and could limit laser pulses.

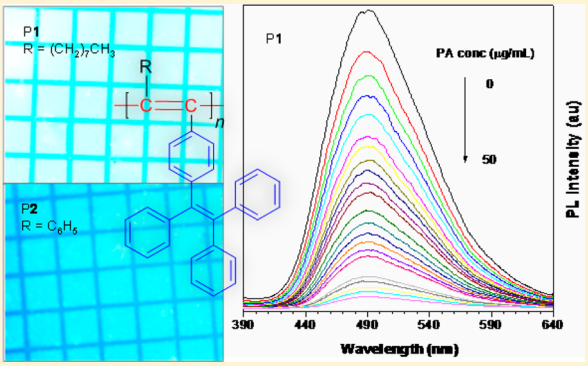

INTRODUCTION

Development of efficient luminophores has attracted considerable interest for their potential applications in organic light-emitting diodes (OLEDs), chemosensors, bioprobes, etc.[1] Many luminophores have been prepared and found to show strong light emission in solutions. However, they become weak emitters or completely nonluminescent when aggregated due to the aggregation-caused quenching (ACQ) effect.[2] In the aggregated state, the luminogenic molecules are in close proximity. This favors the formation of excimers and exciplexes by strong intermolecular interactions and hence led to nonradiative relaxation. This problem must be properly tackled as luminophores are used as solid thin films in their real-world applications. We observed a phenomenon of aggregation-induced emission (AIE), in which aggregate formation is beneficial to the light emission of some molecules such as silole and tetraphenylethene (TPE).[3] Because such a phenomenon is of academic importance and practical signature, many scientists around the world are now doing AIE research. Thanks to their enthusiastic efforts, many new AIE dyes have been created and used for the fabrication of OLEDs with outstanding device performances and served as sensory materials for detecting VOCs, explosives, and biomolecules in high sensitivities and selectivities.[4] However, almost all the AIE luminogens developed so far are low molecular weight molecules and thus are not suitable for the manufacture of large-area flat-panel devices. To solve this problem, one of the best ways is to make their counterparts with high molecular weights, i.e., polymers, which can fabricate into large-area thin solid films through simple processes such as spin coating, static casting, and inkjet printing.

Polyacetylene is a well-known conjugated polymer and exhibits metallic conductivity upon doping. Such discovery has created a new area of research on "synthetic metals".[5,6] Our group has worked on acetylene research for many years and has synthesized many substituted polyacetylenes with advanced materials properties.[7] With the expectation that the resulting polymers will show unique light-emitting properties, we are interested in incorporating AIE molecules into the polyacetylene structures. We had prepared monosubstituted polyacetylenes with silole and TPE luminogens and systematically investigated their optical properties (Chart 1). Whereas the direct attachment of silole pendant to the rigid polyacetylene chain afforded AIE-inactive polymer **P3** due to the poor packing in the aggregated

Received: November 20, 2014
Revised: January 20, 2015

DOI: 10.1021/ma502341j
Macromolecules XXXX, XXX, XXX−XXX

Chart 1. Molecular Structures of Silole and Tetraphenylethene-Containing Monosubstituted Polyacetylenes

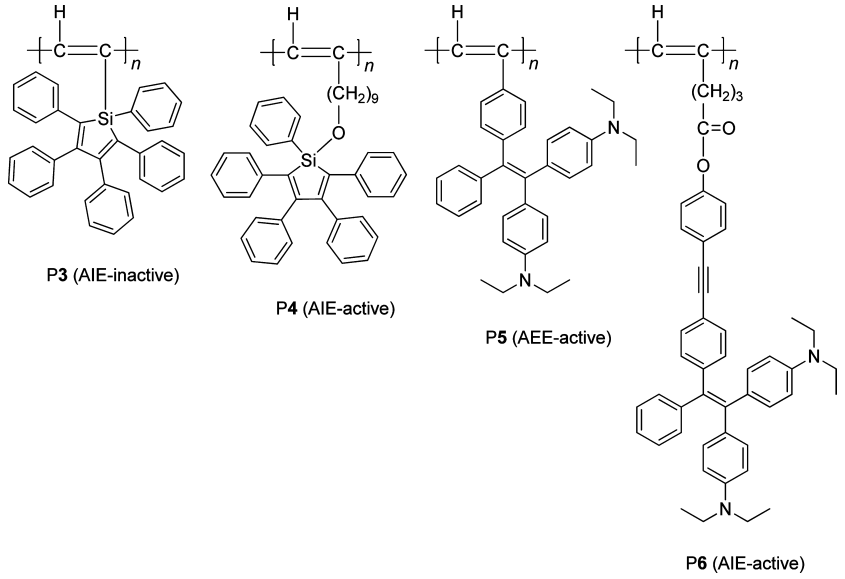

Scheme 1. Synthetic Routes to Tetraphenylethene-Functionalized Acetylenes and Their Polymers

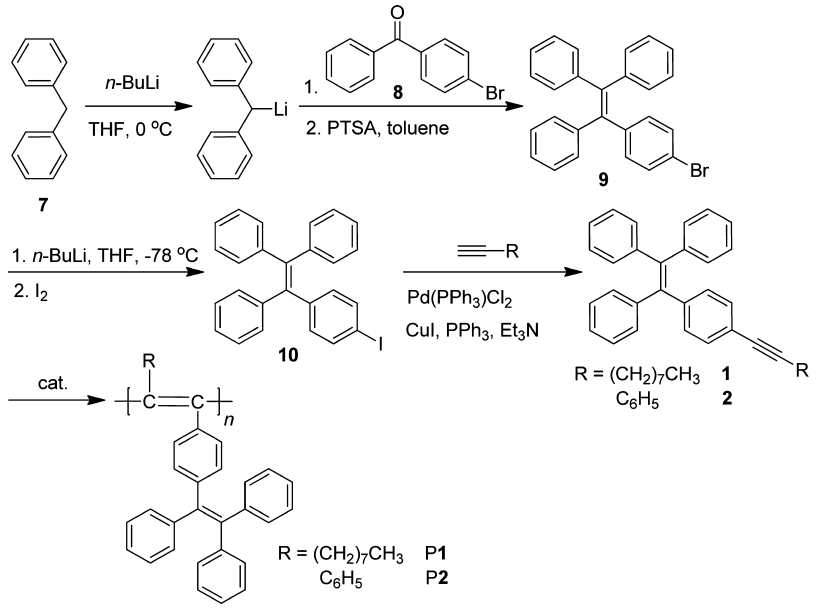

state,[8] polyacetylene **P5** carrying directly linked TPE units exhibited aggregation-enhanced emission (AEE) characteristic.[9] When a flexible alkyl spacer was inserted between the polymer backbone and the pendant group, the motion of the latter was decoupled from the former and hence endowed the resulting polymers **P4** and **P6** with AIE features.[8,9]

Compared with monosubstituted polyacetylenes, disubstituted polyacetylenes generally show higher thermal stability, better film forming and stronger mechanical strength.[10] Although polyacetylene itself is not luminescent, its substituted counterparts can be emissive, with disubstituted polyacetylenes showing stronger light emission than their monosubstituted congeners.[11] Although disubstituted polyacetylenes possess such advantages, they are difficult to prepare, especially those with bulky substituents, due to the comparative low reactivity of their corresponding monomers. In this paper, we take the challenge and intend to prepare disubstituted polyacetylenes carrying AIE luminogens. The electronic communication between the emissive polyacetylene backbone and the AIE unit may confer the resulting polymers with intriguing optical properties. We herein report the synthesis of TPE-functionalized disubstituted polyacetylenes **P1** and **P2** (Scheme 1) and present their properties and their utilization as chemosensors for explosive detection and optical limiters.

EXPERIMENTAL SECTION

Materials and Instrumentation. Tetrahydrofuran (THF) and toluene were freshly distilled from sodium benzophenone and calcium hydride, respectively, under nitrogen. All the chemicals and reagents were purchased from Aldrich and used as received. Weight-average molecular weight (M_w) and polydispersity (M_w/M_n) of the polymers were estimated on a Waters gel permeation chromatography (GPC) system using THF as eluent. Details about the experimental setup can be found in our previous publication.[12]

^{1}H and ^{13}C NMR spectra were measured on a Bruker AV 300 spectrometer using tetramethylsilane (TMS; $\delta = 0$) as internal reference.

DOI: 10.1021/ma502341j
Macromolecules XXXX, XXX, XXX−XXX

High-resolution mass spectra (HRMS) were recorded on a GCT premier CAB048 mass spectrometer operating in MALDI-TOF mode. UV spectra were measured on a Milton Ray Spectronic 3000 Array spectrophotometer. Photoluminescence (PL) spectra were recorded on a PerkinElmer LS 55 spectrofluorometer. Fluorescence quantum yields (Φ_F) of thin films of the polymers were measured on a calibrated integrating sphere. The particle sizes of the polymer aggregates were measured on a Beckman Coulter Delsa 440SX Zeta potential analyzer. Thermogravimetric analysis (TGA) was carried on a TA TGA Q5000 under nitrogen at a heating rate of 10 °C/min. The thermal transitions of the polymers were investigated on a differential scanning calorimeter (DSC) using a TA DSC Q1000 under nitrogen at a heating rate of 10 °C/min. The ground-state geometries were optimized using the density functional (DFT) with B3LYP hybrid functional at the basis set level of 6-31G*. All the calculations were performed using the Gaussian 03 package.

Fluorescence decay curves were recorded on an Edinburgh Instruments FLS920. A femtosecond titanium−sapphire oscillator was used as excitation laser source. The second harmonic (358 nm) of the oscillator output at 716 nm was used for the PL measurement. Time-resolved PL measurements were carried out on a Hamamatsu model C4334 streak camera coupled to a spectrometer. The PL signals were collected at 490 or 510 nm. The decay in the PL intensity with time was fitted by a double-exponential function.[13] The optical nonlinearity of the polymers was investigated by using a frequency-doubled, Q-switched, mode-locked continuum ns/ps Nd:YAG laser. Detailed procedures are described in our previous publication.[14]

Monomer Synthesis. Monomers **1** and **2** were synthesized according to Scheme 1. Detailed procedures are shown below.

Synthesis of 1-(4-Bromophenyl)-1,2,2-triphenylethene (9). To a solution of diphenylmethane (7, 5 g, 29.7 mmol) in dry THF (40 mL) was added 17.7 mL (28.3 mmol) of *n*-butyllithium (2 M solution in hexane) at 0 °C under nitrogen. After stirring for 30 min, 7.4 g (28.3 mmol) of 4-bromobenzophenone (**8**) was added. The reaction mixture was warmed to room temperature. After stirring for another 6 h, the reaction was terminated by addition of an aqueous solution of ammonium chloride. The mixture was extracted with dichloromethane. The organic layer was washed with water and dried over anhydrous magnesium sulfate. After solvent evaporation, the crude alcohol with excess diphenylmethane was then subjected to acid-catalyzed dehydration. The crude alcohol was dissolved in toluene (~50 mL) in a two-necked round-bottom flask equipped with a condenser. After addition of a catalytic amount of *p*-toluenesulfonic acid, the mixture was refluxed for 3−4 h. Afterward, the mixture was washed with 10% aqueous $NaHCO_3$ solution. The organic layer was separated and dried over anhydrous magnesium sulfate. After filtration followed by solvent evaporation, the crude product was purified by silica gel column chromatography using hexane/dichloromethane (9:1 v/v) as eluent. White solid; yield 68% (7.9 g). ^{1}H NMR (300 MHz, $CDCl_3$), δ (ppm): 7.22 (d, 2H), 7.14−7.09 (m, 9H), 7.05−7.00 (m, 6H), 6.89 (d, 2H). ^{13}C NMR (75 MHz, $CDCl_3$), δ (ppm): 143.99, 143.37, 142.27, 140.32, 133.66, 131.95, 131.52, 128.45, 127.35, 121.11. HRMS (MALDI-TOF): m/z 412.0681 [(M + 2)$^+$, calcd 412.0670].

1-[4-(2-Octylethynyl)phenyl]-1,2,2-triphenylethene (1) and 1-[4-(2-Phenylethynyl)phenyl]-1,2,2-triphenylethene (2). 3.8 mL (6 mmol) of *n*-butyllithium (1.6 M in hexane) was added into a THF solution (50 mL) of **9** (2 g, 5 mmol) at −78 °C. After stirring at −78 °C for 2 h, 1.4 g (5.5 mmol) of iodine was added. After stirring at room temperature for another 2 h, water was added and the mixture was extracted with dichloromethane. The organic layer was separated, washed with saturated sodium thiosulfate solution and water, and dried over magnesium sulfate. The mixture was filtrated. After solvent evaporation, the crude product **10** was purified by silica gel column chromatography using hexane as eluent. Into a new 250 mL round-bottom flask was dissolved 3 g (6.5 mmol) of **10** in 50 mL of triethylamine at room temperature. After addition of $Pd(PPh_3)_2Cl_2$ (208 mg, 0.3 mmol), triphenylphosphine (160 mg, 0.6 mmol), CuI (113 mg, 0.6 mmol), and 1-decyne (1.4 g, 10.0 mmol) or phenylacetylene (1.0 g, 10.0 mmol), the mixture was refluxed for 12 h under nitrogen. After solvent evaporation, the residue was extracted with dichloromethane and water. The organic layer was dried over anhydrous $MgSO_4$ and concentrated. The crude product was purified on a silica gel column using hexane as eluent.

Characterization Data for ***1****.* White solid; yield 77% (2.3 g). ^{1}H NMR (300 MHz, $CDCl_3$), δ (ppm): 7.14−7.09 (m, 11H), 7.04−7.01 (m, 6H), 6.93 (d, 2H), 2.37 (t, 2H), 1.44−1.30 (m, 12H), 0.88 (t, 3H). ^{13}C NMR (75 MHz, $CDCl_3$), δ (ppm): 144.28, 144.19, 144.14, 143.76, 141.98, 141.06, 132.04, 131.98, 131.89, 131.95, 131.55, 128.46, 128.35, 128.31, 127.23, 127.19, 122.57, 91.38 (≡*C*−Ph), 81.31 (≡*C*−C_8H_{17}), 32.53, 29.88, 29.81, 29.61, 29.45, 23.34, 20.12, 14.79. HRMS (MALDI-TOF): m/z 468.2380 [M$^+$, calcd 468.2817].

Characterization Data for ***2****.* White solid; yield 90% (2.5 g). ^{1}H NMR (300 MHz, $CDCl_3$), δ (ppm): 7.49 (t, 2H), 7.30−7.28 (m, 6H), 7.12−7.02 (m, 16H). ^{13}C NMR (75 MHz, $CDCl_3$), δ (ppm): 144.20, 143.73, 143.65, 143.56, 141.87, 140.87, 140.48, 131.76, 131.59, 131.55, 131.51, 131.17, 128.55, 128.39, 128.06, 127.95, 127.88, 126.90, 126.82, 126.77, 123.53, 121.26, 89.82 (≡*C*−TPE), 89.79 (≡*C*−Ph). HRMS (MALDI-TOF): m/z 432.2629 [M$^+$, calcd 432.1878].

Polymerization. All the polymerization reactions were carried out under nitrogen. Experimental procedures for the polymerization of **1** are given below as an example.

To a dry Schlenk tube were placed 29 mg (0.05 mmol) of WCl_6 and 22 mg (0.05 mmol) of Ph_4Sn under nitrogen. Dry toluene (3 mL) was injected into the tube, and the tube was then aged at 60 °C for 15 min. Monomer **1** (128.3 mg, 0.18 mmol) was dissolved in 2 mL of anhydrous toluene, and this solution was then transferred to the catalyst solution using a syringe. The resulting mixture was stirred at 60 °C under nitrogen. After 24 h, the mixture was diluted with chloroform and added to a large amount of methanol under stirring via cotton filter to filter, if possible, any insoluble substances. The precipitates were filtered with a Gooch crucible, washed with methanol, and dried under vacuum to a constant weight.

Characterization Data for ***P1****.* Yellow solid; yield 82.2% (Table 1, no. 4). M_w 10 000; M_w/M_n 1.7 (GPC, polystyrene calibration). IR (KBr), υ (cm^{-1}): 3077, 3055, 3023, 2924, 2853, 2068, 1943, 1598, 1492, 1251, 1075, 1030. ^{1}H NMR (300 MHz, $CDCl_3$), δ (TMS, ppm): 7.07, (broad peak), 1.27, 0.90. ^{13}C NMR (75 MHz, $CDCl_3$), δ (TMS, ppm): 144.55, 141.41, 132.06, 128.27, 127.02, 32.60, 30.01, 23.45, 14.87.

Table 1. Polymerization of 1 and 2[a]

entry	catalyst	temp (°C)	yield (%)	M_w[b]	M_w/M_n[b]
		monomer **1**			
1	$NbCl_5$−Ph_4Sn	80	trace		
2	$TaCl_5$−Ph_4Sn	80	8.8	123000	2.3
3[c]	$TaCl_5$−*n*-Bu_4Sn	80	25.4	20700	3.4
4	WCl_6−Ph_4Sn	60	82.2	10000	1.7
5	WCl_6−Ph_4Sn	80	46.0	9200	1.6
6	WCl_6−Ph_4Sn	100	40.5	6700	2.1
		monomer **2**			
7	$TaCl_5$−Ph_4Sn	80	trace		
8[c]	$TaCl_5$−*n*-Bu_4Sn	80	3.3	18000	3.0
9[c]	$TaCl_5$−*n*-Bu_4Sn	100	6.1	4600	1.5
10	WCl_6−Ph_4Sn	80	28.2	3800	1.8
11	WCl_6−Ph_4Sn	100	32.0	5000	2.5
12	WCl_6−Ph_3SiH	80	0		

[a]Carried out under nitrogen in toluene for 24 h. $[M]_0$ = 0.2 M; [cat.] = [cocat.] = 10 mM. [b]Determined by GPC in THF on the basis of a polystyrene calibration. [c][cocat.] = 20 mM.

Characterization Data for ***P2****.* Green solid; yield 28.2% (Table 1, no. 10). M_w 3800; M_w/M_n 1.8 (GPC, polystyrene calibration). IR (KBr), υ (cm^{-1}): 3076, 3052, 3021, 2067, 1946, 1490, 1445, 1251, 1074, 1030. ^{1}H NMR (300 MHz, $CDCl_3$), δ (TMS, ppm): 7.05 (broad peak). ^{13}C NMR (75 MHz, $CDCl_3$), δ (TMS, ppm): 144.44, 141.16, 132.01, 128.26, 126.97.

Fluorescent Photopatterning. Photopatterning was conducted in air at room temperature using 365 nm UV light from a Spectroline ENF-280C/F UV lamp at a distance of 1 cm. The intensity of the

DOI: 10.1021/ma502341j
Macromolecules XXXX, XXX, XXX−XXX

incident light was ~18.5 mW/cm^2. The film was prepared by spin coating the polymer solution (~5 wt % in 1,2-dichloroethane) on a silicon wafer. The polymer film was dried in a vacuum oven and UV-irradiated for 10 min through a copper mask. The fluorescent image of the resulting photopattern was taken on an Olympus BX41 fluorescence optical microscope.

RESULTS AND DISCUSSION

Monomer Synthesis. Two TPE-containing acetylenes (**1** and **2**) were synthesized according to the synthetic routes shown in Scheme 1. Compound **9** was first prepared by coupling reaction of diphenylmethane with 4-bromobenzophenone followed by acid-catalyzed dehydration. It was then converted into its iodinated congener (**10**) by the halogen-exchange reaction. Sonogashira coupling of **10** with 1-decyne and phenylacetylene was catalyzed by $Pd(PPh_3)_2Cl_2$, CuI, and PPh_3 in Et_3N, which furnished the target products **1** and **2** in satisfactory to high yield. All the monomers were carefully purified. Their structures were characterized by standard spectroscopic methods with good results. The ^{1}H and ^{13}C NMR spectra of **1** and **2** are shown in Figures S1−S4 of the Supporting Information.

Polymer Synthesis. Since $NbCl_5$ and $TaCl_5$ are good catalysts for the polymerization of 1-phenyl-1-alkynes[15] and sterically bulky diphenylacetylene derivatives,[16] we thus first tried to use them for the polymerization of **1**. Reaction of **1** in the presence of $NbCl_5$−Ph_4Sn in toluene at 80 °C, however, gave only a small amount of product (Table 1, no. 1). Although a polymer with a high molecular weight was produced using $TaCl_5$−Ph_4Sn as catalyst, the yield was low. Changing the cocatalyst to *n*-Bu_4Sn increased the polymer yield but decreased the molecular weight.

In our previous investigation, we found that WCl_6−Ph_4Sn worked well for the polymerization of diphenylacetylene derivatives.[8] Thus, we tested whether monomer **1** could be polymerized by such catalytic system. Delightfully, after stirring a toluene solution of **1** at 60 °C with WCl_6−Ph_4Sn, a yellow powdery polymer with a satisfactory molecular weight of 10 000 was obtained in a high yield. A further attempt to obtain a better polymerization result by increasing the reaction temperature failed: the isolated yield and molecular weight of the obtained polymer decreased progressively when the polymerization was carried out at 80 and 100 °C.

Monomer **2** displays a polymerization behavior similar to that of **1**. While $TaCl_5$−Ph_4Sn and $TaCl_5$−*n*-Bu_4Sn were generally inactive for the polymerization of **2**, the monomer could be polymerized by WCl_6−Ph_4Sn at 80 °C. It is noteworthy that the molecular weight of **P2** is much lower than **P1**. This is understandable because **2** is sterically more bulky than **1**, which makes the coordination of its molecules to the catalytic active sites a daunting task. Raising the reaction temperature to 100 °C did not help much on the isolated yield and the polymer molecular weight. Further attempt to polymerize **2** by WCl_6−Ph_3SiH was unsuccessful. All the obtained polymers were completely soluble in common organic solvents such as chloroform, dichloromethane, and THF but insoluble in water, hexane, and methanol.

Structural Characterization. Both **P1** and **P2** gave good spectroscopic data corresponding to their molecular structures. Examples of ^{1}H and ^{13}C NMR spectra of **P1** are shown in Figures 1 and 2, respectively, while those of **P2** are given in Figures S5 and S6. For comparison, the spectrum of its monomer **1** was also provided in the same figure. The NMR analysis proved that the acetylene triple bonds of **1** had been converted to the polyene double bonds of **P1** by the polymerization reaction. For example, the ^{1}H NMR spectrum of **P1** showed no peak at δ 2.4 corresponding

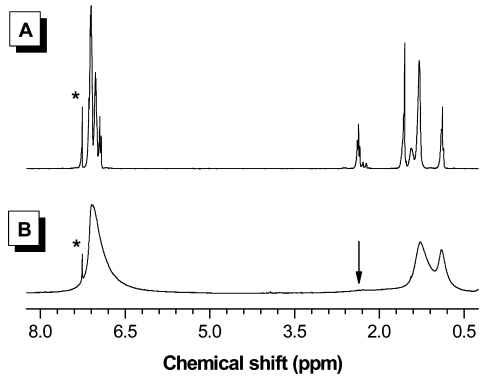

Figure 1. ^{1}H NMR spectra of (A) monomer **1** and (B) its polymer **P1** in chloroform-*d*.

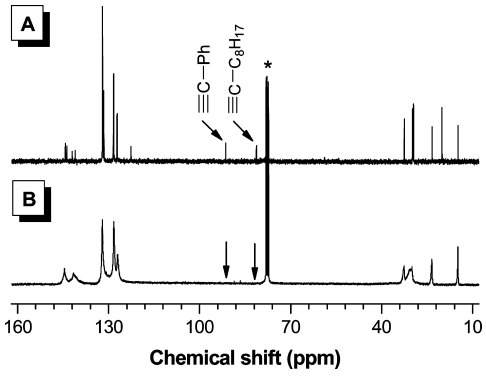

Figure 2. ^{13}C NMR spectra of (A) monomer **1** and (B) its polymer **P1** in chloroform-*d*.

to the absorption of the methylene protons next to the triple bond (≡C−CH_2) of **1**. Its absorption peaks were much broader than those of **1**, which was suggestive of its polymeric character. On the other hand, the acetylenic carbon atoms of **1** absorbed at δ 91.4 and 81.3, which disappeared completely in the spectrum of **P1**. The absorption peaks of the olefinic carbon atoms of the polyacetylene backbone may be overlapped with those of the TPE pendants and are thus not observed.

Thermal Properties. The thermal properties of **P1** and **P2** are investigated by TGA and DSC analyses under nitrogen. Because the majority of the polymers were constructed from aromatic rings, they thus showed outstanding thermal stability (Figure 3). The temperatures for 5% weight loss (T_d) were up to ~400 °C, which were higher than those of **P3**−**P5** (T_d = 350−360 °C), thanks to their more rigid polymer backbone. **P2** showed a higher thermal stability, which was somewhat expected because the aliphatic octyl chain in **P1** had a lower resistance than the phenyl ring in **P2** toward thermolysis. The DSC thermograms of both **P1** and **P2** detected no peaks corresponding to glass transition from room temperature to 300 °C, presumably due to the high rigidity of their disubstituted polyacetylene backbones.

Optical Properties. Figure 4 shows the absorption spectra of **P1** and **P2** as well as their monomers **1** and **2** in THF. Whereas **1** and **2** showed no peaks at wavelengths longer than 410 and 440 nm, the spectra of **P1** and **P2** were well extended to the visible light region up to 530 nm. Clearly, the peaks at the longer wavelengths are due to the absorptions of the double-bond backbones of the polymers. In other words, the polymers are more conjugated than their monomers, thanks to the electronic

DOI: 10.1021/ma502341j
Macromolecules XXXX, XXX, XXX−XXX

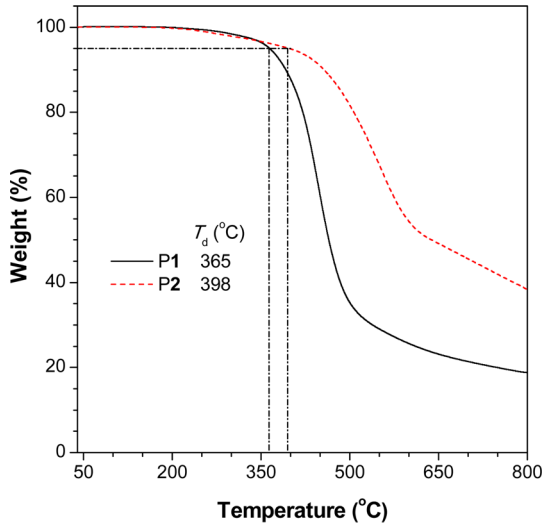

Figure 3. TGA thermographs of **P1** and **P2** recorded under nitrogen at a heating rate of 10 °C/min.

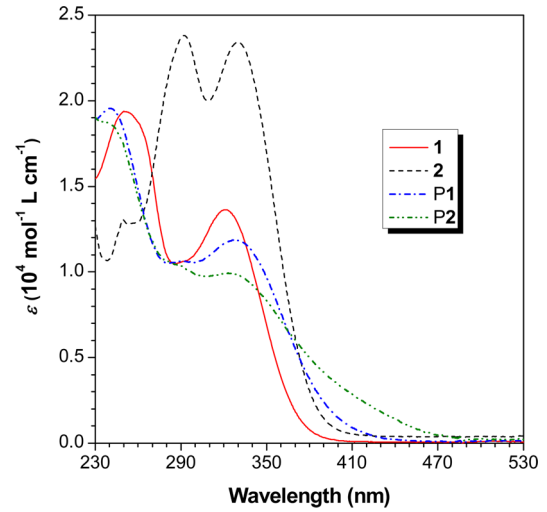

Figure 4. Absorption spectra of **1**, **2**, **P1**, and **P2** in THF solutions. Solution concentration: 10 μM.

communication between the TPE pendants and the polyacetylene backbone. Although **P2** possesses a much lower molecular weight than **P1**, it shows a higher conjugation, as revealed by its longer onset wavelength (470 nm in **P1** and 530 nm in **P2**). This is further substantiated by their appearance: while **P1** is a yellow solid, **P2** appears green in color. The higher conjugation in **P2** may be due to the presence of an additional phenyl ring in the polymer backbone. This also demonstrates that the effective conjugation length of the polymers is rather short, probably owing to the twisting of the polyacetylene chain by the steric repulsion between neighboring substituents.

To better understand their photophysical properties, theoretical calculations on the energy levels of **1** and **2** were carried out. Their highest occupied (HOMO) and lowest unoccupied (LUMO) molecular orbitals plots are given in Figure 5. The HOMO and LUMO of **1** mainly originated from the orbitals of the TPE unit, revealing that its absorption originated mainly from the $\pi-\pi^*$ transition of the TPE component. On the contrary, the orbitals of the HOMO and LUMO of **2** were localized on the whole molecule. This results in an extended conjugation in **2**. The band gap for **1** was calculated to be 3.91 eV, which was wider than that of **2** (3.67 eV). Thus, the theoretical calculation nicely explains the hypsochromic shift in the absorption of **1** from that of **2**.

TPE is practically nonluminescent in solution but becomes highly emissive in the aggregated state. Are the TPE-containing disubstituted polyacetylenes also AIE-active? To answer this, the photoluminescence (PL) of **P1** and **P2** as well as their monomers in THF and THF/H_2O mixtures was investigated. As shown in Figure 6, **P1** was somewhat luminescent at 493 nm in THF (10 μM). The Φ_F was estimated to be 5.2% (Table 2). On the contrary, its monomer **1** is nonemissive under the same measurement conditions. We previously proposed that the AIE effect is caused by the restriction of intramolecular motion, which blocks the nonradiative relaxation channel. Since the TPE units are directly bonded to a rigid polymer skeleton in **P1**, their intramolecular motions are, to some extent, restricted, thus allowing the polymer to emit in the solution state. With a gradual addition of water into the THF solution of **P1**, the PL intensity was progressively enhanced, while the spectral pattern remained almost the same. At 90 vol % water content, the intensity was 4.5-fold higher than that in THF. Since **P1** is insoluble in water, aggregation of its chains should readily occur in THF/H_2O mixtures with high water contents. Clearly, aggregate formation has enhanced the PL of **P1**, or in other words, **P1** is AEE-active. Only a small (6 nm) red-shift in the emission maximum was observed when **P1** was fabricated as solid thin film, which was indicative of weak interactions between polymer strands. Conversely, it exhibited a higher Φ_F value of 7% as measured by a calibrated integrating sphere.

Interestingly, **P2** exhibits a different emission behavior. Like **P1**, its diluted THF solution was emissive and emitted at 511 nm with a Φ_F value of 19.4%. No discernible signals, however, were recorded in the PL spectrum of its monomer. When a small

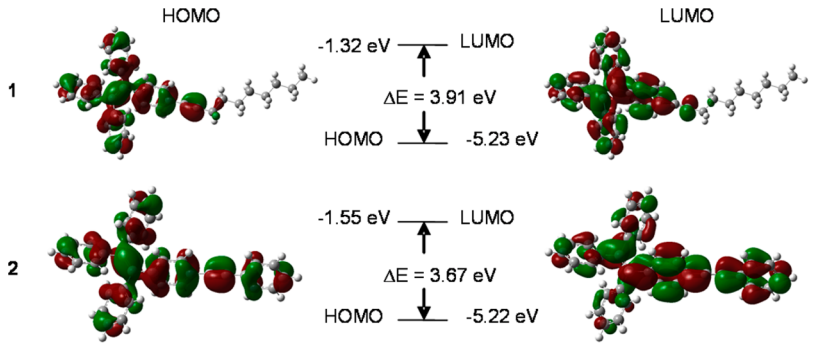

Figure 5. Molecular orbital amplitude plots of HOMO and LUMO levels of **1** and **2** calculated using the B3LYP/6-31G* basis set.

DOI: 10.1021/ma502341j
Macromolecules XXXX, XXX, XXX−XXX

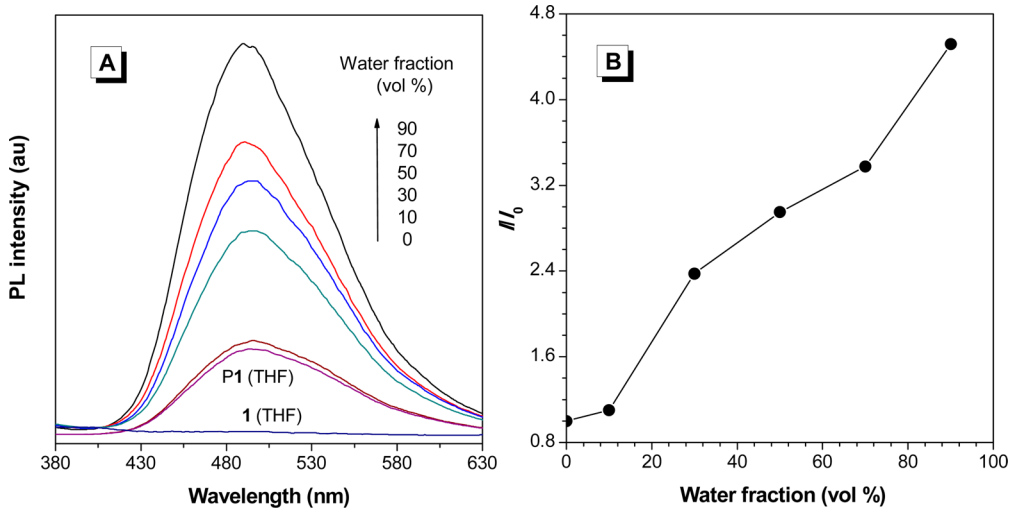

Figure 6. (A) PL spectrum of **P1** in THF and THF/H_2O mixtures with different water fractions. Inset: emission spectrum of **1** in THF solution. Concentration: 10 μM; excitation wavelength: 330 nm. (B) Plot of I/I_0 values versus the compositions of the THF/H_2O mixtures of **P1**.

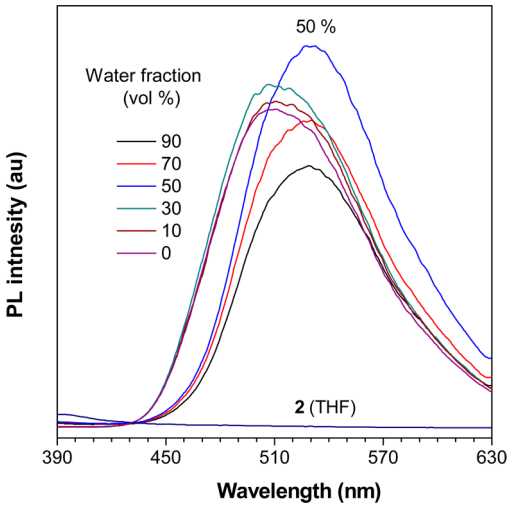

Figure 7. (A) PL spectrum of **P2** in THF and THF/H_2O mixtures with different water fractions. Inset: emission spectrum of **2** in THF solution. Concentration: 10 μM; excitation wavelength: 330 nm. (B) Plot of I/I_0 values versus the compositions of the THF/H_2O mixtures.

Table 2. Absorption and Emission of P1 and P2 in Solution (soln)[a], Aggregate (aggr),[b] and Amorphous (amor) States

	λ_{ab}[c] (nm)	λ_{em}[d] (nm)		
polymer	soln	soln (Φ_F)	aggr	amor (Φ_F)
P1	326	493 (5.2)	496	502 (7.0)
P2	341	511 (19.4)	529	526 (14.1)

[a]In dilute THF solution (10 μM). [b]In THF/H_2O mixtures (1:9 by volume). [c]Absorption maximum. [d]Emission maximum with quantum yields (Φ_F, %) given in the parentheses. The Φ_F values were determined using 9,10-diphenylanthracene (Φ_F = 90% in cyclohexane) as standard (soln) or by a calibrated integrating sphere (amor).

amount of water (<50 vol %) was added to the polymer solution, the emission became stronger progressively. The maximum enhancement was observed at 50% water content. Afterward, the PL intensity dropped along with a red-shift in the emission maximum to 529 nm. The shrinkage in the volume of polymer chain due to the aggregate formation in aqueous mixtures has physically brought the phenyl rings closer. This will increase their $\pi-\pi$ stacking interactions and restrict their intramolecular motions. While the former effect shifts the PL spectrum to the redder region and quenches the light emission, the latter boosts the emission intensity. The competition between the two effects determines the PL behavior of a luminogen. In **P2**, the former effect is prevailed at high water fractions, which thus makes it weakly emissive at the longer wavelength under such circumstance. The Φ_F of its thin film was measured to be 14.1%, which was smaller than its solution value. Thus, unlike **P1**, **P2** exhibits the ACQ effect.

To confirm the formation of polymer particles in THF/H_2O mixtures with high water contents, particle size analyses are carried out. An average size of ~300 nm was detected in 50% aqueous solution of **P1** (Figure 8A). When the amount of water was progressively increased to 70% and then 90%, the sizes of the particles were finally decreased to ~143 nm. At low water fraction, not all the polymer chains are aggregated, and this may allow the dissolved chains to cluster slowly to form "larger" aggregates. On the other hand, the polymer chains may aggregate quickly at high water content, which finally give nanoparticles of "smaller" sizes. A similar phenomenon was also found in **P2**.

Explosive Detection. Detection of explosives has attracted much current interest because of its antiterrorism implications.[17] Among various materials, sensors based on fluorescent conjugated polymers have received much attention, thanks to their signal-amplifying effect and high binding capability to analytes.[18] Because of this, we thus investigated the possibility of the present polymers as fluorescent chemosensors for efficient detection of explosives. Picric acid (PA) was used as a model explosive because of its commercial availability. The polymer aggregates in THF/H_2O mixtures with 50 and 90 vol % water fractions were employed as fluorescent sensors, while the performance of their isolated chains in pure THF was also studied for comparison.

When PA was gradually added into the nanoparticle suspensions of **P1** and **P2** in aqueous mixtures, the PL intensity was progressively decreased but without causing any spectral profile change (Figure 9A and Figure S7 in the Supporting Information). The PL quenching could be recognized at a PA concentration of 1 μg/mL or 1 ppm. At [PA] of 28–50 μg/mL, the emission from the aqueous mixtures was almost quenched completely.

DOI: 10.1021/ma502341j
Macromolecules XXXX, XXX, XXX–XXX

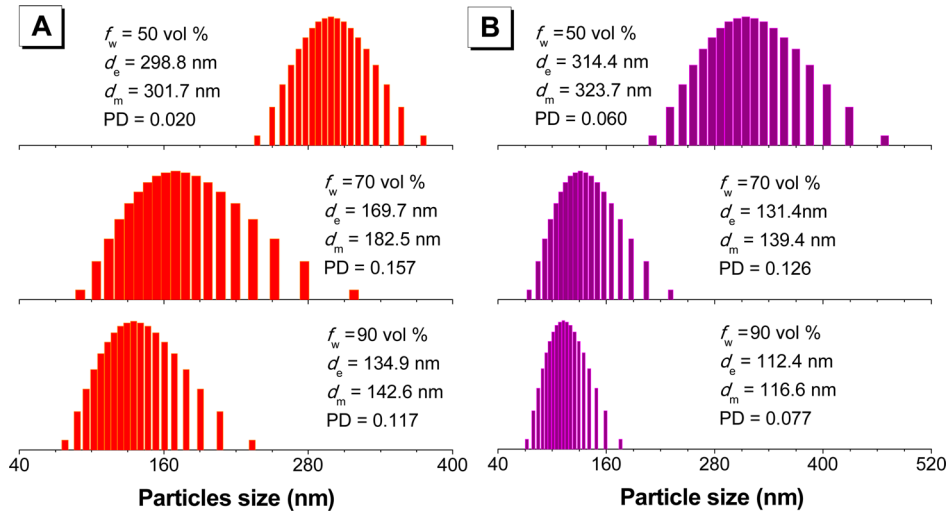

Figure 8. Particle size distributions of aggregates of (A) **P1** and (B) **P2** suspended in THF/water mixtures with water fractions (f_w) of 50, 70, and 90 vol %. Abbreviation: d_e = effective diameter, d_m = mean diameter, PD = polydispersity.

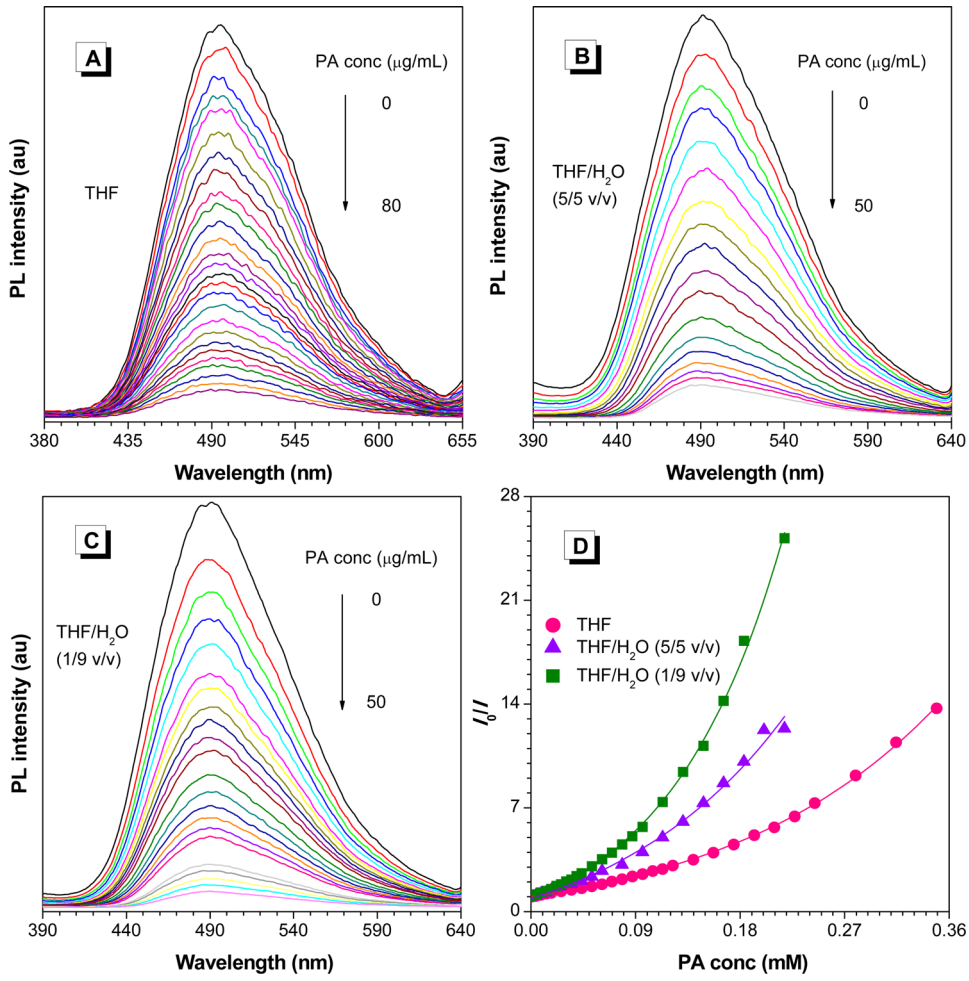

Figure 9. PL spectra of **P1** in (A) THF solution and (B, C) THF/H_2O mixtures with (B) 50 and (C) 90 vol % water contents containing different amounts of picric acid (PA). (D) Plots of I_0/I values versus PA concentrations. I_0 = intensity at [PA] = 0 mM.

The Stern–Volmer plots of relative PL intensity (I_0/I) versus PA concentration reflected the sensing performance and showed upward bent curves instead of straight lines (Figure 9D and Figure S7D). This indicates that the quenching process becomes more efficient or amplified at higher quencher concentration. The PL of the polymers in THF solutions also became weaker upon addition of PA. However, at the same PA concentration, the THF solutions showed stronger emission than the aqueous mixtures, which was indicative of their poorer sensing performance. In our recent publications, the static quenching model is more adequate than the diffusion-controlled dynamic mechanism to describe the PL quenching behaviors by PA.[19] In this

DOI: 10.1021/ma502341j
Macromolecules XXXX, XXX, XXX–XXX

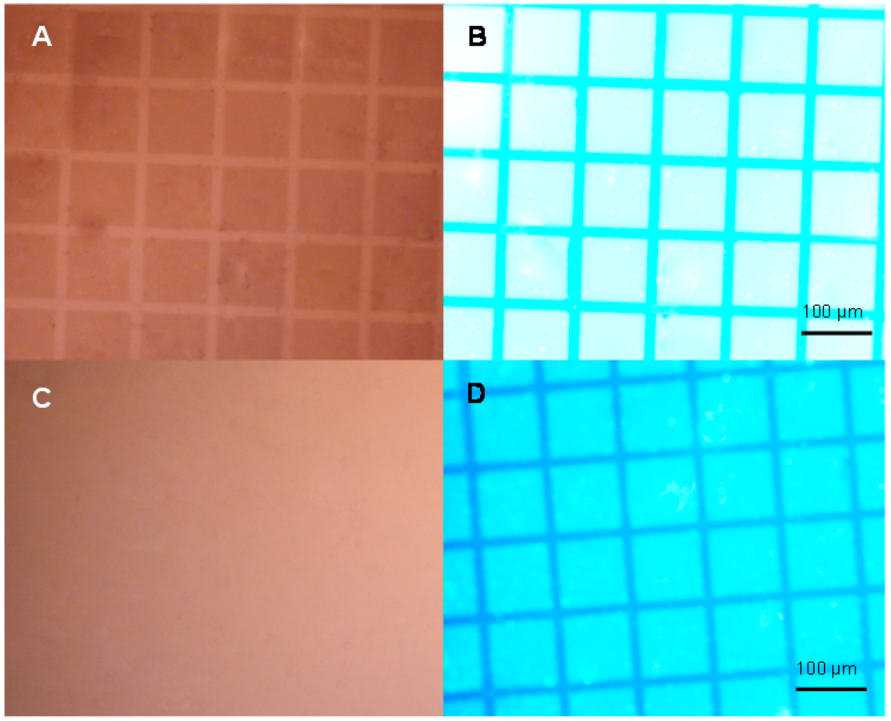

Figure 10. Two-dimensional photopatterns generated by photo-oxidation of films of (A, B) **P1** and (C, D) **P2** on silicon wafers. The photographs were taken under (A, C) normal light and (B, D) UV illuminations.

work, our fluorescent polymers can act as electron donors. The interaction of the PA quenchers with the fluorescent polymers will lead to the formation of nonemissive ground-state dark complexes. The unbound polymers, however, will exhibit their natural lifetimes. On the contrary, in the diffusion-controlled dynamic quenching model, the PL lifetime is shortened with increasing the quencher concentration. To validate which quenching model is involved in the present system, the effect of PA on the lifetime of **P1** and **P2** is investigated. As depicted in Figure S8 and Table S1 of the Supporting Information, the lifetimes of the polymers remained almost unchanged in response to the presence of PA, suggesting that the PL quenching process operated through the static mechanism.

In the static mechanism, the PL annihilation can be described by eq 1.

$$\frac{I_0}{I} = \mathrm{e}^{V_q[\mathrm{PA}]} \tag{1}$$

where I_0 and I are the PL intensities without and with PA, respectively, and V_q is the static quenching constant. Mathematical fitting of the Stern−Volmer plots in Figure 9D and Figure S7D gave eqs 2−7 for **P1** and **P2** in pure THF and THF/H_2O mixtures with 50 and 90% water fractions, respectively:

P1 THF:

$$\frac{I_0}{I} = 2.20\mathrm{e}^{5513[\mathrm{PA}]} - 1.20 \tag{2}$$

THF/water (5/5, v/v):

$$\frac{I_0}{I} = 3.87\mathrm{e}^{6539[\mathrm{PA}]} - 2.99 \tag{3}$$

THF/water (1/9, v/v):

$$\frac{I_0}{I} = 3.06\mathrm{e}^{10089[\mathrm{PA}]} - 2.15 \tag{4}$$

P2 THF:

$$\frac{I_0}{I} = 2.41\mathrm{e}^{4764[\mathrm{PA}]} - 1.39 \tag{5}$$

THF/water (5/5, v/v):

$$\frac{I_0}{I} = 3.07\mathrm{e}^{6369[\mathrm{PA}]} - 2.07 \tag{6}$$

THF/water (1/9, v/v):

$$\frac{I_0}{I} = 3.17\mathrm{e}^{9020[\mathrm{PA}]} - 2.20 \tag{7}$$

Generalization from eqs 2−7 gave eq 8, which was similar to eq 1 but with two extra constants (A and B).

$$\frac{I_0}{I} = A\mathrm{e}^{k[\mathrm{PA}]} + B \tag{8}$$

If these two terms are neglected, the static quenching constants (k) for the solution and aggregated systems of **P1** and **P2** were determined and are summarized in Table S2. In 90% aqueous mixtures, the k values for **P1** and **P2** were 10 089 and 9020 L mol^{-1}, respectively. These values were much higher than those (1−185 L mol^{-1}) of iptycene-containing poly(p-phenyleneebutadiynylene)s and poly(p-phenyleneethynylene)s, which were widely studied fluorescent conjugated polymers for explosive detection.[20] At [PA] → 0, eq 8 can be transformed to eq 9, which can be rearranged to give eq 10 with $K = Ak$ and $C = A + B = 1$.

$$\frac{I_0}{I} = A\left(1 + k[\mathrm{PA}] + \frac{1}{2}k^2[\mathrm{PA}]^2 + \ldots + \frac{k^n[\mathrm{PA}]^n}{n!} + \ldots\right) + B \tag{9}$$

$$\frac{I_0}{I} = A(1 + k[\mathrm{PA}]) + B = Ak[\mathrm{PA}] + A + B = K[\mathrm{PA}] + C \tag{10}$$

DOI: 10.1021/ma502341j
Macromolecules XXXX, XXX, XXX−XXX

Thus, the static quenching constant (K) of **P1** in 90% aqueous mixture at low PA concentration was 30 872 L mol^{-1}, which was 2.5 times larger than the value in pure THF solution (12 129 L mol^{-1}). The K value for **P2** in 90% aqueous mixture was also reasonably high (28 593 L mol^{-1}), being also 2.5-fold larger than that in THF (11 481 L mol^{-1}). All these values were much higher than those of chemosensors based on polymetalloles, whose K values fell in the range from 6710 to 11 000 L mol^{-1}.[21] The higher quenching constants in aqueous mixtures revealed a amplification effect in the nanoaggregated system. Such an effect is presumably due to the AEE characteristics of the polymers and/or the presence of many internal voids for capturing PA molecules and more migration channels available to excitons in the polymer aggregates. These factors work cooperatively to endow the system with sensitive response to PA. Conjugated polymers **P1** and **P2** are good promising materials for the construction of fluorescent chemosensors with amplified responses and extremely low detection limits.

Fluorescent Photopatterning. Light-driven techniques are more convenient due to their simple operation and precise control on the curing reaction and patterning process. On the other hand, creation of fluorescent patterns is important to the construction of photonic and electronic devices and the development of biological sensing and probing systems. Both **P1** and **P2** possess good processability and can form thin films by spin-coating of their solutions. They are also emissive in the aggregated state. These enable the fabrication of fluorescent photopattern by photolithography process. Indeed, when the thin films of **P1** and **P2** were exposed to UV light through copper masks in air for 10 min, the exposed parts were photo-oxidized and their emission was quenched, while the masked regions (emissive squares) remained emissive. Without going through the development process, two-dimensional fluorescent patterns were thus generated (Figure 10). The nonirradiated parts of the patterned film of **P1** emitted blue light, whose intensity was so strong that it appeared white under UV illumination (Figure 10B).

Optical Limiting. Previous studies found that polymers constructed from aromatic acetylenic monomers can limit optical power.[22] **P1** and **P2** contain numerous aromatic rings, and they are thus anticipated to exhibit interesting optical limiting properties. Figure 11 shows the optical limiting performance of **P1** and **P2** in chloroform at similar linear transmittance (T = ~30%). The transmitted fluence of the polymers increased initially with increasing the incident fluence but started to deviate from linearity at a value of ~1 J/cm^2. When the incident fluence was further strengthened, the transmitted fluence reached a plateau and saturated at 0.4 J/cm^2. Clearly, both **P1** and **P2** can limit laser pulses. Together with their novel properties described before, they are expected to find many high-technological applications.

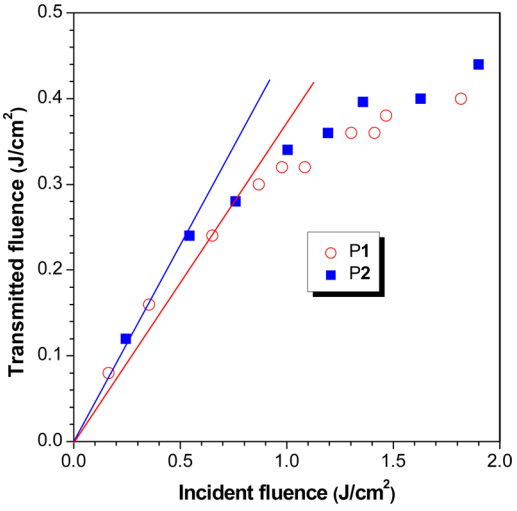

Figure 11. Optical limiting responses to 35 ps, 532 nm optical pulses of chloroform solutions of **P1** and **P2**. Concentration: 0.2 mg/mL.

CONCLUSIONS

In this work, disubstituted acetylenes with directly linked TPE pendants were synthesized and polymerized by WCl_6–Ph_4Sn in toluene at elevated temperatures, producing polymers **P1** and **P2**. The polymers possessed good solubility and showed high thermal stability. Both polymers were weak emitters in the solution state. Whereas the PL of **P1** was enhanced by aggregate formation, that of **P2** was quenched. The polymers could detect explosives sensitively with an amplification effect. They were sensitive to UV irradiation and were promising materials for fabricating fluorescent photopatterns. The polymers exhibited optical nonlinearity and could limit laser pulses.

ASSOCIATED CONTENT

Supporting Information

^{1}H and ^{13}C NMR spectra of **1**, **2**, and **P2**, PL spectra of **P2**, PL decay curves, fluorescence decay parameters, and quenching constants for explosive detection. This material is available free of charge via the Internet at http://pubs.acs.org.

AUTHOR INFORMATION

Corresponding Author

*(B.Z.T.) E-mail tangbenz@ust.hk; Ph +852-2358-7375 (8801); Fax +852-2358-1594.

Notes

The authors declare no competing financial interest.

ACKNOWLEDGMENTS

This work has been partially supported by the National Basic Research Program of China (973 Program; 2013CB834701), the National Science Foundation of China (21490570 and 21490574), the Research Grants Council of Hong Kong (604913, 604711, 602212 and N_HKUST620/11), and the University Grants Committee of Hong Kong (AoE/P-03/08). B.Z.T. thanks the support of the Guangdong Innovative Research Team Program (201101C0105067115).

REFERENCES

(1) (a) Feast, W. J.; Cacialli, F.; Koch, A. T. H.; Daik, R.; Lartigau, C.; Friend, R. H.; Beljonne, D.; Brédas, J. L. *J. Mater. Chem.* **2007**, *17*, 907–912. (b) Friend, R. H.; Gymer, R. W.; Holmes, J. H.; Marks, R. N.; Taliani, C.; Bradley, D. D. C.; Dos Santos, D. A.; Brédas, J. L.; Lösdlund, M.; Salaneck, W. R. *Nature* **1999**, *397*, 121–128.

(2) Birks, J. B. *Photophysical of Aromatic Molecules*; Wiley: London, 1970.

(3) (a) Luo, J.; Xie, Z.; Lam, J. W. Y.; Cheng, L.; Chen, H.; Qiu, C.; Kwok, H. S.; Zhan, X.; Liu, Y.; Zhu, D.; Tang, B. Z. *Chem. Commun.* **2001**, 1740–1741. (b) Tang, B. Z.; Zhan, X.; Yu, G.; Lee, P. P. S.; Liu, Y.; Zhu, D. *J. Mater. Chem.* **2001**, *11*, 2974–2978.

(4) For reviews on aggregation-induced emission, please see: (a) Hong, Y.; Lam, J. W. Y.; Tang, B. Z. *Chem. Soc. Rev.* **2011**, *40*, 5361–5388. (b) Zhao, Z.; Lam, J. W. Y.; Tang, B. Z. *Curr. Org. Chem.* **2010**, *14*, 2109–2132. (c) Liu, J.; Lam, J. W. Y.; Tang, B. Z. *J. Inorg.*

DOI: 10.1021/ma502341j
Macromolecules XXXX, XXX, XXX–XXX

Organomet. Polym. Mater. **2009**, *19*, 249−285. (d) Hong, Y.; Lam, J. W. Y.; Tang, B. Z. *Chem. Commun.* **2009**, 4332−4353. (e) Li, K.; Liu, B. *Chem. Soc. Rev.* **2014**, *43*, 6570−6597. (f) Qu, H. H.; Jiang, L. L.; Chen, T.; Hu, Z. C.; Deibert, B. J.; Li, J. *Chem. Soc. Rev.* **2014**, *43*, 5815−5840. (g) Zhang, X.; Yin, J.; Yoon, J. *Chem. Rev.* **2014**, *114*, 4918−4959. (h) Zhang, J. J.; Zou, Q.; Tian, H. *Adv. Mater.* **2013**, *25*, 378−399. (i) Zhao, G. S.; Shi, C. X.; Guo, Z. Q.; Zhu, W. H.; Zhu, S. Q. *Chin. J. Org. Chem.* **2012**, *32*, 1620−1632. (j) Qu, H. H.; Jiang, L. L.; Chen, T.; Tang, J. K. *Chin. J. Org. Chem.* **2014**, *34*, 1061−1073. (k) Chen, M. J.; Yin, M. Z. *Prog. Polym. Sci.* **2014**, *39*, 365−395. (l) Mei, J.; Hong, Y.; Lam, J. W. Y.; Qin, A. J.; Tang, Y. H.; Tang, B. Z. *Adv. Mater.* **2014**, *26*, 5429−5479.

(5) (a) Shirakawa, H. *Angew. Chem., Int. Ed.* **2001**, *40*, 2575−2580. (b) MacDiarmid, A. G. *Angew. Chem., Int. Ed.* **2001**, *40*, 2581−2590. (c) Heeger, A. J. *Angew. Chem., Int. Ed.* **2001**, *40*, 2591−2611.

(6) (a) Akagi, K. *Chem. Rev.* **2009**, *109*, 5354−5401. (b) Masuda, T. *J. Polym. Sci., Part A: Polym. Chem.* **2007**, *45*, 165−180. (c) Huang, C. H.; Yang, S. H.; Chen, K. B.; Hsu, C. S. *J. Polym. Sci., Part A: Polym. Chem.* **2006**, *44*, 519−531.

(7) (a) Liu, J.; Lam, J. W. Y.; Tang, B. Z. *Chem. Rev.* **2009**, *109*, 5799−5867. (b) Lam, J. W. Y.; Tang, B. Z. *Acc. Chem. Res.* **2005**, *38*, 745−754.

(8) Chen, J.; Xie, Z.; Lam, J. W. Y.; Law, C. C. W.; Tang, B. Z. *Macromolecules* **2003**, *36*, 1108−1117.

(9) Yuan, W.; Zhao, H.; Shen, X.; Mahtab, F.; Lam, J. W. Y.; Sun, J.; Tang, B. Z. *Macromolecules* **2009**, *42*, 9400−9411.

(10) (a) Lam, J. W. Y.; Tang, B. Z. *J. Polym. Sci., Part A: Polym. Chem.* **2003**, *41*, 2607−2629. (b) Masuda, T.; Tang, B. Z.; Higashimura, T.; Yamaoka, H. *Macromolecules* **1985**, *18*, 2369−2373.

(11) (a) Sanda, F.; Nakai, T.; Kobayashi, N.; Masuda, T. *Macromolecules* **2004**, *37*, 2703−2708. (b) Lam, J. W. Y.; Dong, Y.; Cheuk, K. K. L.; Luo, J.; Xie, Z.; Kwok, H. S.; Mo, Z.; Tang, B. Z. *Macromolecules* **2002**, *35*, 1229−1240. (c) Huang, Y. M.; Lam, J. W. Y.; Cheuk, K. K. L.; Ge, W.; Tang, B. Z. *Macromolecules* **1999**, *32*, 5976−5978.

(12) Chan, C. Y. K.; Tseng, N. W.; Lam, J. W. Y.; Liu, J.; Kwok, R. T. K.; Tang, B. Z. *Macromolecules* **2013**, *46*, 3246−3256.

(13) Chan, C. Y. K.; Zhao, Z.; Lam, J. W. Y.; Liu, J.; Chen, S.; Lu, P.; Mahtab, F.; Chen, C.; Sung, H. H. Y.; Kwok, H. S.; Ma, Y.; Williams, I. D.; Wong, K. S.; Tang, B. Z. *Adv. Funct. Mater.* **2012**, *22*, 378.

(14) Liu, J.; Lam, J. W. Y.; Jim, C. K. W.; Ng, J.; Cheuk, Y.; Shi, J.; Su, H.; Yeung, K. F.; Hong, Y.; Mahtab, F.; Yu, Y.; Wong, K. S.; Tang, B. Z. *Macromolecules* **2011**, *44*, 68−79.

(15) Teraguchi, M.; Masuda, T. *Macromolecules* **2002**, *35*, 1149−1151.

(16) Masuda, T.; Higashimura, T. *Adv. Polym. Sci.* **1987**, *81*, 121−165.

(17) (a) Liu, Y.; Mills, R. C.; Boncella, J. M.; Schanze, K. S. *Langmuir* **2001**, *17*, 7452−7455. (b) Kim, T. H.; Kim, H. J.; Kwak, C. G.; Park, W. H.; Lee, T. S. *J. Polym. Sci., Part A: Polym. Chem.* **2006**, *44*, 2059−2068. (c) Sanchez, J. C.; Trogler, W. C. *J. Mater. Chem.* **2008**, *18*, 3143−3156. (d) Naddo, T.; Che, Y.; Zhang, W.; Balakrishnan, K.; Yang, X.; Yen, M.; Zhao, J.; Moore, J. S.; Zhang, L. *J. Am. Chem. Soc.* **2007**, *129*, 6978−6979. (e) Germain, M. E.; Knapp, M. J. *J. Am. Chem. Soc.* **2008**, *130*, 5422−5423. (f) Hughes, A. D.; Glenn, I. C.; Patrick, A. D.; Ellington, A.; Anslyn, E. V. *Chem.—Eur. J.* **2008**, *14*, 1822−1827. (g) Jiang, Y.; Zhao, H.; Zhu, N.; Lin, Y.; Yu, P.; Mao, L. *Angew. Chem., Int. Ed.* **2008**, *47*, 8601−8604. (h) Long, Y.; Chen, H.; Yang, Y.; Wang, H.; Yang, Y.; Li, N.; Li, K.; Pei, J.; Liu, F. *Macromolecules* **2009**, *42*, 6501−6509.

(18) (a) Thomas, S. W., III; Joly, G. D.; Swager, T. M. *Chem. Rev.* **2007**, *107*, 1339−1386. (b) Zahn, S.; Swager, T. M. *Angew. Chem., Int. Ed.* **2002**, *41*, 4225−4230. (c) Bunz, U. H. F. *Chem. Rev.* **2000**, *100*, 1605−1644.

(19) (a) Liu, J.; Zhong, Y.; Lu, P.; Hong, Y.; Lam, J. W. Y.; Faisal, M.; Yu, Y.; Wong, K. S.; Tang, B. Z. *Polym. Chem.* **2010**, *1*, 426−429. (b) Lu, P.; Lam, J. W. Y.; Liu, J.; Jim, C. K. W.; Yuan, W.; Xie, N.; Zhong, Y.; Hu, Q.; Wong, K. S.; Cheuk, K. K. L.; Tang, B. Z. *Macromol. Rapid Commun.* **2010**, *31*, 834−839.

(20) Zhao, D.; Swager, T. M. *Macromolecules* **2005**, *38*, 9377−9384.

(21) Sohn, H.; Sailor, M. J.; Magde, D.; Trogler, W. C. *J. Am. Chem. Soc.* **2003**, *125*, 3821−3830.

(22) (a) Haussler, M.; Liu, J.; Zheng, R.; Lam, J. W. Y.; Qin, A.; Tang, B. Z. *Macromolecules* **2007**, *40*, 1914−1925. (b) Peng, H.; Cheng, L.; Luo, J. D.; Xu, K. T.; Sun, Q. H.; Dong, Y. P.; Salhi, F.; Lee, P. P. S.; Chen, J. W.; Tang, B. Z. *Macromolecules* **1999**, *32*, 2569−2576.

DOI: 10.1021/ma502341j
Macromolecules XXXX, XXX, XXX−XXX